Helicity in the formation of turbulence

Cite as: Phys. Fluids **19**, 025101 (2007); https://doi.org/10.1063/1.2375077
Submitted: 06 July 2006 . Accepted: 02 September 2006 . Published Online: 27 February 2007

D. D. Holm, and R. M. Kerr

Helicity in the formation of turbulence

D. D. Holm
Imperial College, United Kingdom and Los Alamos National Laboratory, Los Alamos, New Mexico 87545

R. M. Kerr
School of Engineering, University of Warwick, Coventry CV4 7AL, United Kingdom

(Received 6 July 2006; accepted 2 September 2006; published online 27 February 2007)

Helicity in vortex structures and spectra is studied in the developmental stages of a numerical simulation of the Navier-Stokes equations using three-dimensional visualizations and spectra. First, time scales are set using the growth and decay of energy dissipation, the peak value of vorticity, and the helicity. Then, two stages between the early time, nearly inviscid Euler dynamics with vortex sheets and a final state of fully developed turbulence with vortex tubes, are described. In the first stage, helicity fluctuations develop in Fourier space during a period still dominated by vortex sheets and rapidly growing peak vorticity. At the end of this period the strongest structure consists of transverse vortex sheets with mixed signs of helicity. During the second stage, a dissipative interaction propagates along one of these vortices as the sheets roll each other into vortex tubes.
 [DOI: 10.1063/1.2375077]

I. INTRODUCTION

It remains an open question how, starting from smooth initial conditions, the Navier-Stokes equations generate turbulence with an ensemble of localized vortex structures that are smooth only on the smallest scales, and possibly not even there. Insight into this process can be gained by simulating initially smooth flows that evolve into turbulence. Past work has tended to focus either on the initial development or on the final state. Very little analysis has been done on the transition to the final state. This paper will focus upon that transition in a single numerical flow from its initial development, through a transition, and finally into fully developed turbulence.

In the classical phenomenological description of the turbulent transfer of energy from large to small scales, one assumes that the dynamics is essentially inviscid at large scales, that energy is transferred to small scales through a cascade, and then is finally dissipated at those small scales. The classical theory then predicts, using dimensional arguments, that the kinetic-energy spectrum should go as $E(k) \sim k^{-5/3}$ in the "inertial subrange" of wavenumbers. While the vortex tubes that dominate the final state are strongly helical, a phenomenological role for helicity in the turbulence cascade has not yet been identified.

The phenomenology of this cascade and its spectra assumes that a mechanism for producing small-scale turbulence exists. The equations tell us that this is through the production of mean square vorticity or enstrophy and vortex stretching. But what about cases where the initial conditions are smooth and strong vortex stretching has not formed? How might the intermediate state following the initial instabilities determine the intermittent structures seen in realistic flows? The problem studied here looks, in detail, at what can occur if the initial instabilities generate large-scale vortex sheets or shear layers. This is true in many physical flows including flow over an obstacle that sheds vorticity and around the edges of thermally driven plumes. The development of this state could determine how rapidly the strong vortex stretching develops and the intermittent turbulent state that follows.

The initial condition used here and in several other papers was chosen because its development covers all the stages from a smooth but energetic state, to fully turbulent flow. It will be shown that in this case, the transformation of these sheets into vortex tubes occurs through the interactions between structures not individually through rollup. We will tie this to the large localized values of helicity that develop, both in physical space and in Fourier space, before tubes are formed. We will propose that interacting vortex structures of oppositely signed helicity underlie the topological changes observed and that this process is inherently dissipative. The primary analysis tools used to describe the transition will be three-dimensional (3D) graphics and helicity cospectra.

The paper is organized as follows. It will be shown through direct numerical simulation (DNS) that this flow is consistent with the picture that large-scale vortex sheets end as small-scale turbulence dominated by vortex tubes with a $-5/3$ energy spectrum. The transition will then be discussed in three parts. Section III discusses the stage immediately after the first formation of vortex sheets and before $T=0.5$ in terms of helicity dynamics in the Euler equations and helicity cospectra. It is during this stage that the transverse, helical vortex sheets that led to the reinvestigation of this flow first appear. In Sec. IV the structure of the two transverse, helical vortex sheets at $T=0.5$ is described in detail. Section V discusses the self-annihilation of these structures after $T=0.5$. These steps demonstrate one mechanism by which small-scale dissipation and vortex tubes can form from smooth initial conditions. We will conclude with a comparison between a traditional view of how the turbulent cascade forms and what this analysis suggests.

Although only one case is presented, other flows in the literature will be discussed in which similar events have been

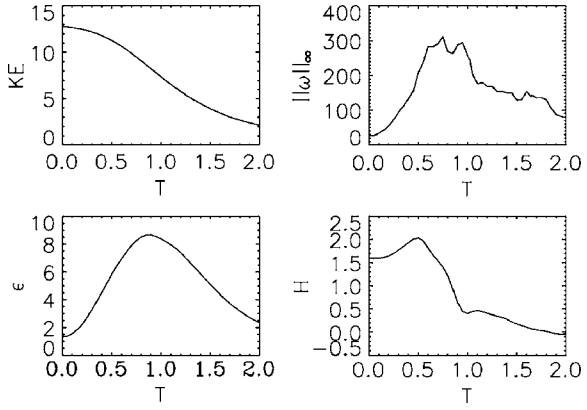

FIG. 1. Time dependence of kinetic energy KE, $\|\boldsymbol{\omega}\|_\infty$, dissipation ϵ, and integral helicity H for our 256^3 direct numerical simulation. The time scale is set by the first peak in $\|\boldsymbol{\omega}\|_\infty$ around $T=0.5$.

observed. Depending upon how common the events are, some aspects of the transition might be universal and therefore might be relevant to the general statistical problem in turbulence.

II. BACKGROUND

Simulations of the initial stages in the Navier-Stokes generation of turbulence can be divided into two categories: those that rapidly form vortex sheets and those that are initialized with smooth, localized vortex tubes. The initial value problem is closely related to whether the incompressible Navier-Stokes equations

$$\partial_t \boldsymbol{u} + (\boldsymbol{u}\cdot\nabla)\boldsymbol{u} = -\nabla P + \nu\nabla^2\boldsymbol{u},$$
$$\nabla\cdot\boldsymbol{u} = 0, \tag{1}$$

are "regular."[1] For $\nu=0$, the Euler equations, this is only possible if the time integral of the maximum vorticity $\|\boldsymbol{\omega}\|_\infty$ becomes infinite.[2] The folklore is that Navier-Stokes solutions are regular. Whether the equations are singular would have a dramatic effect upon the nature of any transition from smooth initial conditions to a turbulent flow, but this will not be the topic of the present paper. The focus here will be the first stage in the extension to viscous flows.

For the Euler equations, if the initial state is smooth at the largest scales, vortex sheets quickly appear that suppress singularities and there is only exponential growth in the maximum vorticity.[3,4] If the initial state is composed not of sheets, but of smooth, localized vortex tubes with finite energy in finite domains, a growing body of evidence from numerical simulations indicates that the 3D Euler equations form antiparallel vortices and could have singularities.[5–7] In all of these cases, the indications are that the singular behavior begins only after the most intense vorticity organizes itself into an antiparallel configuration. For a more generic initial condition that develops vortex sheets, the focus of this paper, the picture is less clear.

The Euler equations conserve two quadratic invariants,

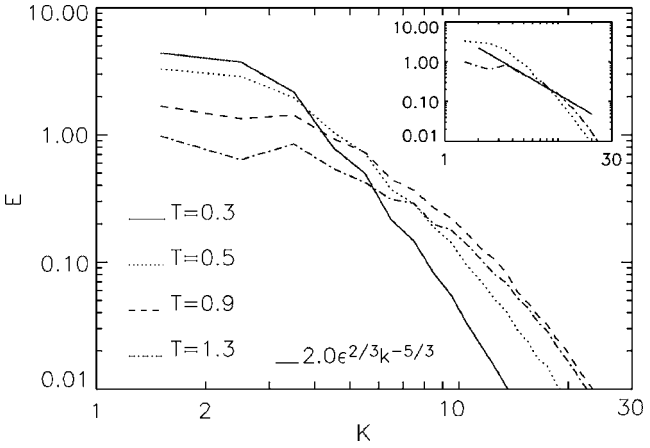

FIG. 2. Comparison of the energy spectra vs the three-dimensional wavenumber $k=(k_x^2+k_y^2+k_z^2)^{1/2}$ in shells of width $\Delta k=1$ for several times. The initial energy was in wavenumbers $|k|\leq 4$, and quickly fills all shells with a very steep spectrum. After $T=0.5$, an inertial range spectrum gradually forms, becoming firmly established by $T=1.3$ as shown by the inset, where the straight line is $E(k)=2\epsilon^{2/3}k^{-5/3}$.

$$\text{energy}\quad \mathrm{KE} = \frac{1}{2}\int \boldsymbol{u}^2 dV,$$
$$\text{helicity}\ H = \int h(x)dV = \int \boldsymbol{u}\cdot\boldsymbol{\omega}dV, \tag{2}$$

where $\boldsymbol{\omega}=\nabla\times\mathbf{u}$ is the vorticity and $h(x)=\mathbf{u}(x)\cdot\boldsymbol{\omega}$ is the local helicity density. For the Navier-Stokes equations in a periodic box, the dissipation of the energy ϵ is related to the enstrophy or mean square vorticity Ω by

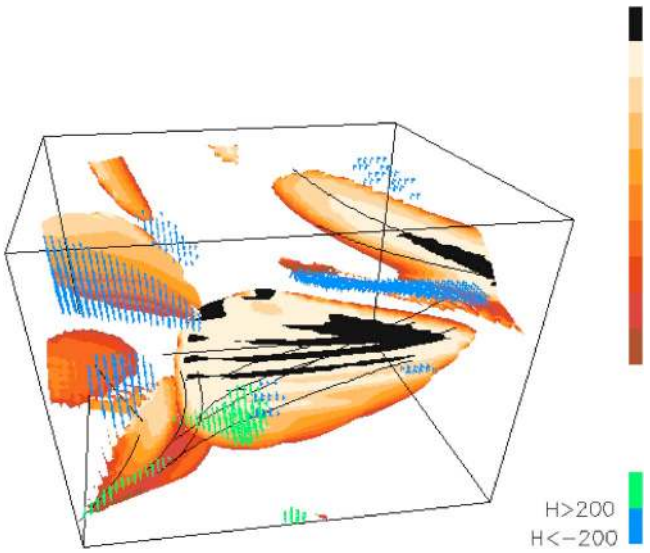

FIG. 3. Vorticity isosurfaces in the entire domain at an early time ($T=0.3$) when the flow is dominated by vortex sheets. $\|\omega\|>0.47\|\boldsymbol{\omega}\|_\infty$, $\theta_y=100^\circ$. In all of the three-dimensional figures the vorticity isosurface color scale is the red earth tones in the upper part of the color bar. Hashes show where helicity magnitude is large with blue representing $h<0$ and green $h>0$. In gray-scale, the darker hashes are $h<0$ and the lighter hashes are $h<0$. A red cross (not in this figure) will indicate the position of $\|\boldsymbol{\omega}\|_\infty$ at the given time. Lines are vortex lines originating at randomly chosen points within regions of large $\|\boldsymbol{\omega}\|_\infty$.

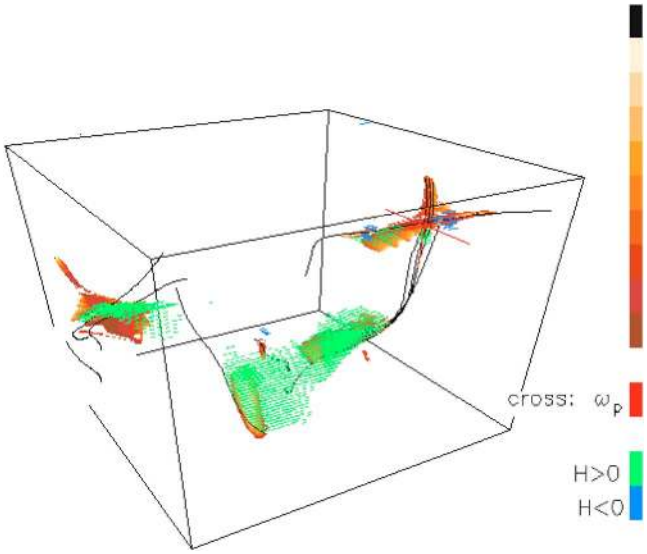

FIG. 4. Vorticity isosurfaces at $t=0.5$ for $1/2^3$ of the domain. $\|\boldsymbol{\omega}\| > 0.55\|\boldsymbol{\omega}\|_\infty$ and $\theta_y=30^\circ$. The maximum vorticity $\|\boldsymbol{\omega}\|_\infty$ is within the cross at the upper right. The interaction to be followed in Figs. 9–11 between $T=0.5$ and 0.7 will start with this cross, then proceed down the bundle of vortex lines coming out of it and into the connected green $h>0$ structure.

$$\partial_t \mathrm{KE} = \epsilon = \nu\Omega = \nu \int \omega^2 dV. \tag{3}$$

While KE and H remain constant for the three-dimensional Euler equations, the enstrophy will grow due to vortex stretching.

Fully developed turbulence is found numerically either in forced simulations or at late times in decaying turbulence. It was shown as early as 1980 (G. S. Patterson, private communication) that these flows generated vortex tubes, as documented in Refs. 8 and 9. It was not until later[10] that the possible importance of alternative structures was realized. This would include vortex sheets, often interacting in configurations where their vorticity vectors were nearly orthogonal. We shall refer to these interacting structures as "transverse vortex sheets" and one such structure will be the focus of this paper.

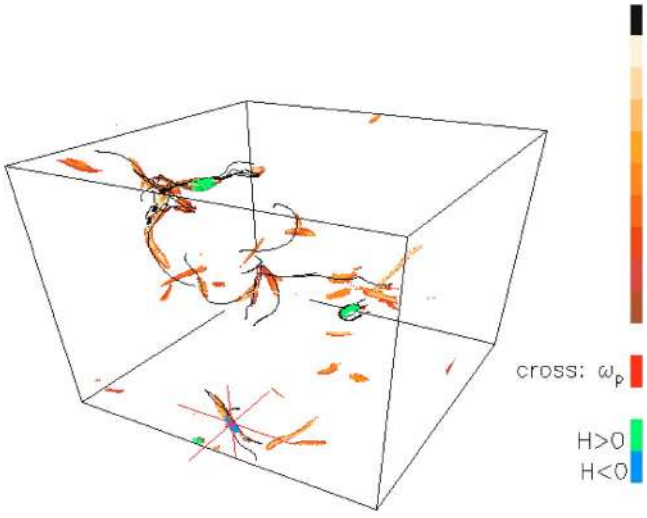

FIG. 5. Vorticity isosurfaces at $T=0.7$, the end of the transition to vortex tubes, for the entire domain. $|\omega|>0.39\|\boldsymbol{\omega}\|_\infty$ and $\theta_y=330°$. To study vortex dynamics near $\|\boldsymbol{\omega}\|_\infty$, the region at the lower front edge will be magnified in subsequent figures.

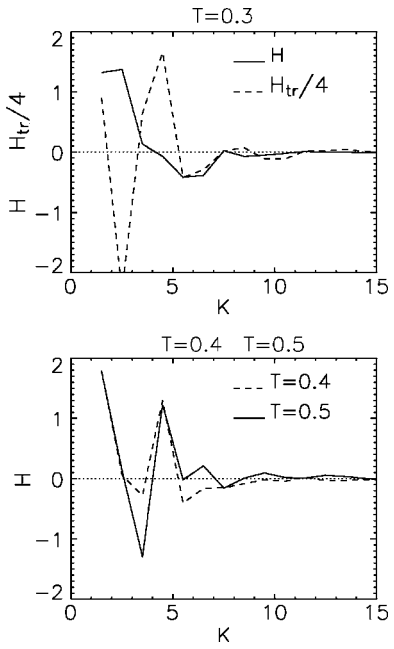

FIG. 6. Helicity spectra $H(k)$ at $t=0.3$, 0.4, and 0.5 and a helicity transfer spectrum $H_{tr}(k)$ at $t=0.3$. Most of the change in the helicity spectrum occurs between $t=0.3$ and $t=0.4$, the period during which in physical space regions of negative and positive helicity density emerge, as shown in Fig. 9. Note the relationship between the oscillations in $H(k)$ at $t=0.5$ and the oscillations in $H_{tr}(k)$ at $t=0.3$. The high negative and positive transfer rates at $t=0.3$ result in the changes seen in the helicity spectrum at $t=0.4$.

For the Reynolds numbers accessible to such simulations, all the expected statistics of grid turbulence in a wind tunnel[11] are observed. This includes a $-5/3$ spectrum,[9] $E(k)=C_k\epsilon^{2/3}k^{-5/3}$, the velocity derivative skewness[12] $\overline{(\partial u/\partial x)^3}/\overline{(\partial u/\partial x)^2}=-0.5$, and anomalous scaling of higher-order statistics.[10]

The transition between the initial and final states has not been studied previously in great detail, perhaps because the transition is not expected to be universal. It would be universal if the structures and statistics were representative of the statistical state of fully developed turbulence. The objective of this paper is to begin to fill this gap by discussing in detail the structural changes during this transition for one generic flow. This will start from the smooth initial condition proposed earlier for decaying isotropic turbulence by Ref. 13. The initial condition used in Ref. 13 consisted of low-wavenumber Fourier modes ($|k|\leqslant 4$) with a nearly uniform spectrum and random phases. High-wavenumber amplitudes were initially set to zero in order to prevent them from obscuring the development of the low-wavenumber modes.

This initial condition has been discussed in two previous papers.[13,14] The purpose of the first study[13] was to demonstrate the initial formation of vortex sheets and the eventual appearance of fully developed turbulence. The purpose of the second study[14] was originally to provide a basis for comparisons with large-eddy simulations (LES), but instead we de-

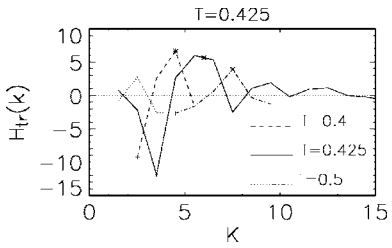

FIG. 7. Helicity transfer spectra. The full transfer spectrum $H_{tr}(k)$ at $T=0.425$ is shown along with segments of the $T=0.3$ and 0.5 transfer spectra to show how the spectrum appears to move to higher wavenumbers as time progresses. The peak positives are marked with (⋆) and the peak negatives are marked with (+).

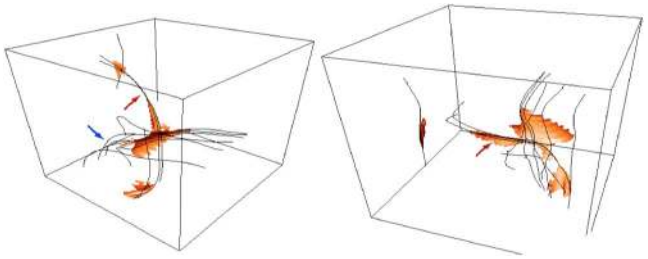

FIG. 8. Isosurfaces of vorticity and vortex lines at $T=0.5$ for the $1/4^3$ subdomain centered on $\|\boldsymbol{\omega}\|_\infty$ in the upper right of Fig. 4. The isosurfaces in the two perspectives of $\theta_y=50°$ and 160° emphasize the sheet-like character, while the vortex lines show the beginnings of tube-like concentrations. The vertical structure in the $\theta_y=50°$ perspective is the same as the horizontal structure on the left of the $\theta_y=160°$ perspective as indicated by the red arrows. Note the twisted vortex lines on the left-hand side of the sheet for $\theta_y=50°$ and indicated by the blue arrow. The red (upper) and blue (lower) arrows in this and the following two figures point to the same structures. As the vortex structures naturally wrap around each other, these twisted vortex lines will evolve into the blue vortex tube at later times.

cided to focus upon the appearance of helical transverse sheets. LES comparisons with this initial condition have since been done by two other groups.[15,16] The LES comparisons show that a full description of the behavior of this idealized DNS is relevant to engineering applications.

Time scales. Figure 1 shows the time dependence of kinetic energy KE, maximum vorticity $\|\boldsymbol{\omega}\|_\infty$, dissipation $\epsilon=\int dV\nu|\nabla u|^2$, and integral helicity H (6). The time interval $0<t<1$ covers approximately one eddy turnover time. The most important time in the analysis to be presented is $t\approx 0.5$, the first peak in the maximum of the vorticity, the L_∞ norm denoted as $\|\boldsymbol{\omega}\|_\infty$. Energy spectra have also been traditionally used to set time scales. Figure 2 details how the spectrum evolves from energy only in the lowest Fourier modes at $T=0$ until a short $-5/3$ regime appears at $T=1.3$, with $C_k=2$, which is consistent with the standard coefficient of $C_k\approx 1.7$ given that the Reynolds number is low ($R_\lambda=70$ at $T=1.3$).

Once the time scales are set, the local transitional structures are studied in detail. Vortex sheets, as seen most clearly in Fig. 3, dominate the flow from $T=0$ up to $T\approx 0.5$. For $T<0.4\|\boldsymbol{\omega}\|_\infty$ is growing steadily but not sharply, then between $T=0.4$ and 0.5, $\|\boldsymbol{\omega}\|_\infty$ increases sharply, then stops growing abruptly, with another slightly greater peak in $\|\boldsymbol{\omega}\|_\infty$ at $T=0.7$. The transition from a flow dominated by vortex sheets to one dominated by vortex tubes is completed during $0.5<T<0.9$. After $T=0.9$ the flow satisfies the classical definition of fully developed turbulence. Namely, the following conditions hold: $\|\boldsymbol{\omega}\|_\infty$ and energy are decaying, vortex tubes dominate the structures, and the spectrum is evolving towards the short $-5/3$ slope at $T=1.3$.

Some evidence for these regimes is also seen in the other time curves in Fig. 1. Dissipation ϵ grows steadily between the time that vortex sheets initially form at $T\approx 0.3$ until the end of the transition period, with $d\epsilon/dt$ largest for $T\approx 0.5$. Helicity first becomes more positive in the period before $T=0.5$, then steadily becomes more negative during the transition period between $T\approx 0.5$ and $T\approx 0.9$. The mechanism for this trend is discussed in detail in Sec. V.

Sequence of events. The overall change in the three-dimensional appearance is summarized by Figs. 3–5 at $T=0.3$, 0.5, and 0.7, respectively. Figures 3 and 5 each show the entire domain at the beginning and end of the the time span to be considered, while Fig. 4 focuses upon the $1/2^3$ subdomain over which the primary transition in structure will occur. Figure 3 at $T=0.3$ is clearly dominated by vortex sheets. The major fine-scale structure at $T=0.5$ is also composed of vortex sheets, but these sheets have now acquired strong helicity variations and at the larger scales are clearer starting to form tubes. By $T=0.7$ in Fig. 5, the most intense structures are sparser helical vortex tubes. Figures 6 and 7 use a variety of helicity spectra to show how these helicity variations evolve in Fourier space up to $T=0.5$. Figures 8–11 for $T=0.5$ to 0.7 focus upon the lower front edge of Fig. 5 identified by the red cross. The objective is to identify how the sheets at $T=0.5$ in Fig. 4 change into tubes by $T=0.7$.

III. FORMATION OF TRANSVERSE HELICAL STRUCTURES

A new feature this paper will focus upon is the growth and decay of helicity in interacting vortices. While the time dependence of total helicity in Fig. 1 shows that there is some smooth, large-scale residual helicity in the initial condition, it will be the production of small-scale helicity that will be dynamically important. This is most easily seen at early times ($T<0.5$) in fluctuations in the helicity cospectra, which will be the focus of this section.[17]

The appearance of helicity fluctuations for $T\leqslant 0.5$ is not associated with a large overall change in the total helicity H of the flow, which can only occur through dissipation. Changes in both H and kinetic energy KE for $T\leqslant 0.5$ are small, implying that the inviscid Euler equations should apply. Without dissipation, how can the Euler equations generate large amounts of local helicity density?

The *helicity density* $h=\mathbf{u}\cdot\boldsymbol{\omega}$ in the Navier-Stokes equations obeys

$$\partial_t h+\boldsymbol{u}\cdot h=-\boldsymbol{\omega}\cdot\nabla\Pi+\nu\Delta h-2\nu\mathrm{tr}(\nabla\boldsymbol{\omega}\cdot\nabla\boldsymbol{u}^T). \tag{4}$$

Neglecting the viscous terms, there is advection on the left- and right-hand sides, a source $-\boldsymbol{\omega}\cdot\nabla\Pi=\nabla\cdot\boldsymbol{\omega}\Pi$ when the vorticity is aligned with the gradient of the pressure head $\Pi=p-1/2u^2$. Since the right-hand side is a divergence, global helicity in a periodic domain will be conserved by the Euler equations. This term exists only along vortex lines and

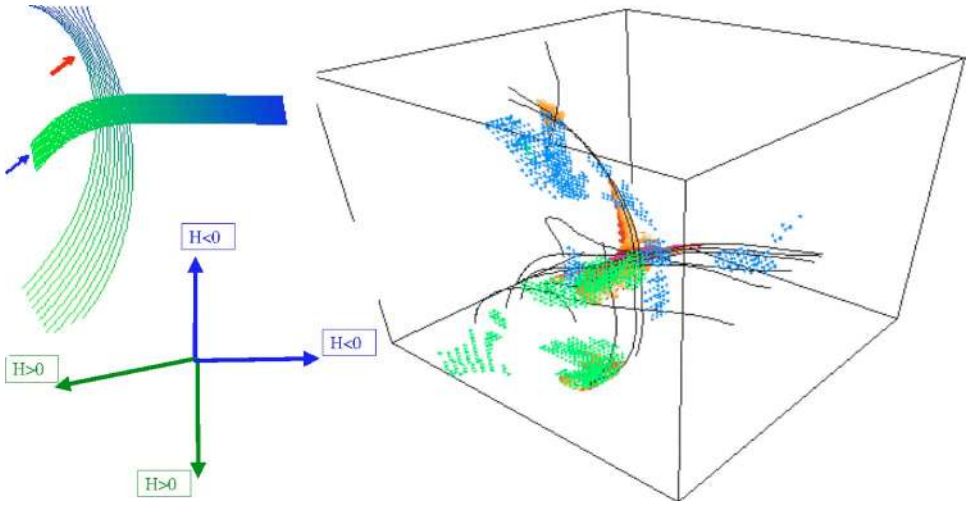

FIG. 9. Vorticity isosurfaces at $T=0.5$. The cube shown is a $1/4^3$ domain with $|\omega|>0.55\|\boldsymbol{\omega}\|_\infty$ and $\theta_y=50°$. The diagrams on the left indicate how helicity density of opposite signs (blue and green) has been expelled in opposite directions along each bundle of vortex lines. In grayscale: darker gray=blue is $h<0$, lighter gray=green is $h>0$, and darkest=black is $h\approx 0$. Figure 8 shows that the vortex structures have not fully changed from sheets into tubes and therefore are represented by transitional ribbons, with one over the other. For the overlying ribbon, its green $h>0$ left end corresponds to the green blotch in the center of the cube while this ribbon's blue $h<0$ right end corresponds to the furthest right blue in the cube. For the underlying ribbon, its blue upper end corresponds to the uppermost blue of the cube and its green lower end corresponds to the lower, central green of the cube and the long green $h>0$ structure in Fig. 4.

generates locally polarized helicity along these lines.

Three types of helicity cospectra have been looked at: the helicity cospectrum $H(k)$, the nonlinear helicity transfer $H_{tr}(k)$, and the helicity dissipation $H_\epsilon(k)$:

$$H(k)=\int \mathrm{d}\Omega\Delta k\boldsymbol{u}(k)\cdot\boldsymbol{\omega}(k)\quad (a),$$

$$H_{tr}(k)=\int \mathrm{d}\Omega\Delta k\mathbf{N}(\mathbf{k})\cdot\boldsymbol{\omega}(\mathbf{k})\quad (b), \tag{5}$$

$$\mathbf{H}_\epsilon(\mathbf{k})=2\nu\int \mathrm{d}\Omega\Delta\mathbf{k}\mathbf{k}^2\omega(\mathbf{k})\quad (c),$$

$\mathbf{N}(\mathbf{k})$ is the Fourier transform of the physical space nonlinear term $-(\mathbf{u}\cdot\nabla)\mathbf{u}-\nabla p$ in the Navier-Stokes equation (1) and $\mathrm{d}\Omega$ is for the integration over solid angle. In our numerical simulation these are defined on spherical shells of width $\Delta k=1$, and k is the average magnitude of a wavenumber within a shell. The spectra have the following properties:

$$H=\int \mathrm{d}kH(k)=\int \mathrm{d}Vu(x)\cdot\omega(x)\quad \text{is conserved when } \nu=0,$$

$$\mathrm{d}H\mathrm{d}t=-H_\epsilon=-\int \mathrm{d}kH_\epsilon(k), \tag{6}$$

$$\int \mathrm{d}kH_{tr}(k)=0\quad \text{due to helicity conservation.}$$

Only H and H_{tr} are plotted.

The physical space equation (4) has been used to explain the appearance of nearly maximal helicity in the inviscid

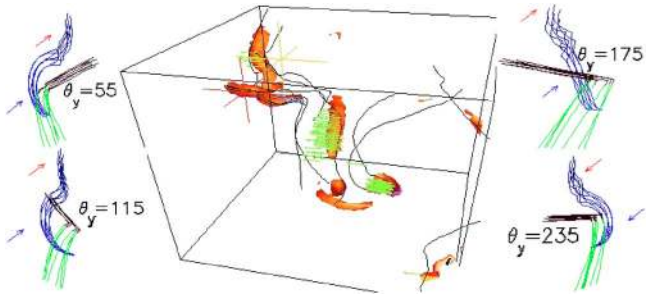

FIG. 10. Isosurfaces of vorticity for $|\omega|>0.5\|\boldsymbol{\omega}\|_\infty$ and helicity at intermediate time $t=0.6$. The cube is for $1/2^3$ of the domain from the perspective of $\theta_y=165°$. The position of $\|\boldsymbol{\omega}\|_\infty$ at the earlier time $t=0.5$ is indicated by the light yellow cross, and the position of $\|\boldsymbol{\omega}\|_\infty$ at $t=0.6$ is indicated by the darker red cross. The surrounding diagrams cover a range of perspectives and are discussed in detail in the Appendix. The upper left diagram at $\theta_y=55$ corresponds to the perspective in Fig. 9 and the perspective of the cube is between the perspectives at $\theta_y=115$ and 175. The red and blue arrows refer to where these ends came from at $T=0.5$ in Fig. 8.

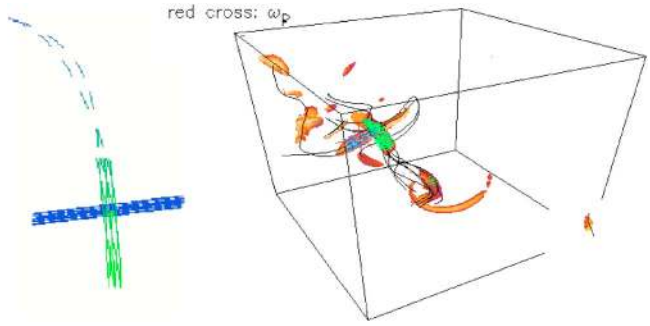

FIG. 11. Isosurfaces of vorticity $|\omega|>0.39\|\boldsymbol{\omega}\|_\infty$ and helicity at $t=0.7$ for $1/2^3$ of the domain at $\theta_y=210°$, rotated 180° from Fig. 4. The position of the $\|\boldsymbol{\omega}\|_\infty$ at $t=0.5$ is in the upper left corner and has now dissipated. The transverse structure that was a sheet at $t=0.5$ has been transformed into the blue ($h<0$, darker gray) tube. The dashed line in the diagram on the left indicates where there were vortex structures at $T=0.5$, which have now been dissipated.

interaction of two antiparallel vortices.[18] In that calculation, the nearly singular interaction generates helicity of opposite signs in the two directions around the point of maximum vorticity. There is no requirement that the vortices be antiparallel to produce this effect, only an expectation that there be strongly interacting vortices. This is illustrated by the inset of Fig. 9. Due to symmetries, in a strictly antiparallel configuration the two signs of physical space helicity would cancel in Fourier space at each wavenumber and thus preclude any spectral oscillations. This should also hold over the wavenumbers of a simulation that correspond to physical space length scales where vortex filaments might be evolving towards an antiparallel configuration.

Figure 6 shows helicity fluctuations in Fourier space growing during the period $0.3<T<0.5$, which is the first sign that this calculation might not see antiparallel vortex structures. Strong fluctuations in $H_{tr}(k)$ appear around $T=0.3$ and are the source of the fluctuations in $H(k)$ for $0.3<T<0.5$, and probably physical space helicity in Figs. 3 and 4. The spontaneous appearance of $H(k)$ is similar to what was observed when symmetries were used to create maximally helical modes of opposite sign.[19] In those cases, helicity of opposite sign appeared in adjacent wavenumber bands, with the higher band dissipating after appearing to propagate to still higher wavenumbers. This contrasts with simulations with only one sign of helicity in the largest modes, which suppress the energy cascade.[20] No physical space structure was identified with these spectral space events.

Changes in the global helicity can only occur through the dissipation of helicity of the opposite sign. This suggests a relationship between the destruction of high wavenumber spectral fluctuations of $H(k)$ in Fig. 6 and the destruction small-scale, helical, physical space structures such as those around the primary structure in Fig. 9. This identification is possible because there is only one small-scale helical structure at this time. The trends in Fig. 1 (lower right frame) are that H becomes more positive for $T<0.5$, then decreases for $T>0.5$. Our interpretation of these changes is as follows.

For $T<0.5$ the slight increase in the helicity is associated with the decrease, then change in sign of the negative Fourier space peak around $k=6$ between $T=0.4$ and $T=0.5$ in the lower frame of Fig. 6. The decrease in positive H for $T>0.5$ is associated with the positive Fourier space helicity peaks at higher wavenumbers at $T=0.5$.

In physical space, these changes appear to be associated with the destruction of structures. First, there is the annihilation of the two blue ($h<0$) regions seen in Fig. 9 but not seen in Fig. 10, a process that probably began before $T=0.5$ and would account for $dH/dt>0$ for $T<0.5$. The decrease in positive H for $T>0.5$ would be associated in physical space with the annihilation of the dominant green ($h>0$) region in Fig. 4 and to be discussed further using Figs. 9–11. The proper diagnostic for dissipation of helicity would be the furthest right term in (4) and will be investigated in a future study.

The final point we wish to make about the spectra is that, for $T\leqslant 0.4$, these fluctuations are only significant for $k\leqslant 6$. There are virtually no fluctuations in either the helicity or the helicity transfer for $k>6$ until $T\approx 0.425$. Figure 7 shows that starting then, the positive and negative peaks in the helicity transfer spectrum appear to propagate to higher wavenumbers.[21] Our best graphics suggest that the major topological change that produces the structure in the upper-right-hand side of Fig. 4, and in Fig. 9, occurs near $T=0.425$. Further calculations with better resolution and higher Reynolds numbers will hopefully answer this question.

IV. DETAILS AT $T=0.5$

It was when rotating the structure in Fig. 9 at $T=0.5$, which is at the height of the transition, that the authors first realized[14] that these interacting structures could never be described as antiparallel and are largely sheet-like during the transition process. The fluctuations in helicity spectra just discussed would be consistent with the observation of transverse structures. Several perspectives and fields are used here to describe the vortex structures in detail, emphasize what the dynamics between $T=0.3$ and $T=0.5$ has created, and understand where the dissipation for $0.5<T<0.7$ is coming from. Diagrams have been added to some of the figures to emphasize these points.

Figure 8 shows two views of the $1/4^3$ subdomain around the peak vorticity without helicity hashes in order to emphasize that at the height of the transition process, sheets are still dominant, although the sheets are much finer than those seen at $T=0.3$. The first perspective is roughly the same as in Fig. 4 and exactly the same as in Fig. 9. The second perspective is roughly the same as in Fig. 10. Arrows are used to show which twisted vortex lines will evolve into the blue vortex tube at later times.

Figure 9 includes two diagrams alongside the figure from our earlier work. The inset of just lines demonstrates how the polarized helicity that is generated in the region of closest interaction is expelled as the vortex lines are stretched out. The left diagram is to show how the two transverse structures slightly wrap around each other. It is important to realize that the upper branch, indicated by the red arrow, actually bends far back, as seen in the 160° perspective in Fig. 8. The diagram also shows that along each vortex sheet, opposite signs of helicity are concentrated along either end of the structures. $h>0$ appears to be concentrated on the left of the horizontal structure and the bottom of the vertical structure, while $h<0$ is at the right and top.

The structures in Fig. 9 connect through the green at the bottom to the significant long green structure across the center of Fig. 4. Going back to Fig. 4, the strongest interaction for $T>0.5$ will work its way down the vortex lines overlaid with green that leads out of structure in the upper right. This same subdomain is used in Figs. 10 and 11. In the process, the remaining vortex sheets will turn into helical vortex tubes and then be annihilated.

V. ANNIHILATION

We now propose that the increases of energy and helicity dissipation near $T=0.5$ in Fig. 1 are due to the self-annihilation of the structure being discussed. This will be illustrated through three-dimensional visualizations and dia-

grams in Figs. 9–11. The three-dimensional visualizations in Figs. 10 and 11 are of the same $1/2^3$ subdomain as in Fig. 4, but from different angles. The diagrams on the left are designed to simplify the process as it might be viewed from a single rotating perspective. The three frames and respective times are chosen so as to represent the following stages: the start of the dissipation process at $T=0.5$ when the structures are still sheet-like; the height of reconnection at $T=0.6$; and the end of the strongly dissipative period at $T=0.7$. The dominant structures at $T=0.7$ are nearly orthogonal vortex tubes with different signs of helicity.

The process starts with the nearly orthogonal vortex sheets described in the last section. The tangle of partially reconnected vortex lines in the upper left of the $T=0.6$ visualization in Fig. 10 arises in the next step in the evolution. All the sheets have turned into tubes and virtually all the signs of strong helicity have disappeared. Exceptions are the green in the middle, which is from the same structure that is in the middle of Fig. 4 at $T=0.5$, and the blue tip next to it, which is discussed below.

Four perspectives of a cartoon are included to help unravel which parts from $T=0.5$ are reconnecting to each other. The cartoon uses three primary colors: green for $h>0$, blue for $h<0$, and black for neutral helicity $h\sim 0$. The details are given in the Appendix and can be summarized as follows: (1) Reconnection of the ends of the original vortices with oppositely signed helicity. [2(a)] Helicity is neutralized (black in diagrams) before the structures are completely annihilated. [2(b)] Vortex tubes form. (3) New helicity with the sign opposite to that in the remaining major structure appears. (4) Interactions between structures with oppositely signed helicity continue.

The manner in which segments with oppositely signed helicity reconnect is similar to what would happen in antiparallel reconnection.

Figure 11 shows the final step in the annihilation of the structure at $T=0.7$. The blue tip, which was beginning to be pulled out at $T=0.6$, is now behind the original green vortex. By $T=0.7$ all the vortex sheets that were originally in the vicinity of $\|\boldsymbol{\omega}\|_\infty$ at $T=0.5$ have either been annihilated or turned into vortex tubes. Figure 1 shows that this is the period during which dissipation is largest. The maximum vorticity $\|\boldsymbol{\omega}\|_\infty$ is located in these structures until $t\approx 0.8$.

VI. DISCUSSION AND OPEN QUESTIONS

When viewed at very close range, the crossed, maximally helical vortex tubes at $T=0.7$ appear as isolated structures,[14] which would be consistent with the classic picture of apparently isolated, helical vortex tubes that have appeared in renderings going back to the mid-1980s including Refs. 3, 9, 22, and 10. The point here is that when viewed from further out in Fig. 11 (and still further back in Fig. 5), and after following where they came from, we know that the vortices are not isolated and are instead strongly interacting. At no time during this calculation are the most intense vorticity elements observed to be antiparallel, and oscillations in the helicity cospectra, impossible for antiparallel vortices, begin at an early time.

TABLE I. Two scenarios for the creation of vortex tubes out of smooth, random initial conditions. The (A) scenario on the left is based upon simulations of interacting vortex tubes. The (B) scenario on the right is based upon simulations that use smooth initial conditions. The (B) scenario seems to apply to the present case.

Stages	
(1) Collision of blobs	
(2) Appearance of vortex layers (sheets)	
$T=0.25T_e$	
[3(A)]	[3(B)]
(a) Enhanced rollup	(a) Transverse vortex configuration
Vortex tubes	(b) Expulsion of helicity, reconnection
Antiparallel attraction	and week dissipation while vorticity
(b) $\lim_{\nu\to 0}\lim_{t\to T_c}\|\omega\|_\infty\to\infty$	is steel in layer and $\|\omega\|_\infty$ is growing
(c) Reconnection:	(c) Formation of vortex tubes and
Viscous dissipation	strong dissipation
(d) Isolated tubes	
(4) Small-scale vortex tubes. $E(k)\sim k^{-5/3}$	
$T=T_e$	

This is a recurring process. Once the punch has gone from the interaction of these structures, a new sheet-like interaction begins to dominate the dynamics. This begins as the immature sheets structure on the left of Fig. 4 at $T=0.5$, develops into the structures in the upper-left-hand side of Fig. 5 at $T=0.7$, and is responsible for the second peak in $\|\boldsymbol{\omega}\|_\infty$ near $t=1.0$ in Fig. 1. Similar transitions has been observed, but not dissected, in graphics for earlier simulations.[9,10] If these events have a common structure, it suggests that the dynamics for the transition here might be more universal than previously supposed and relevant to the statistical state of fully developed turbulence. It could be that the statistics related to the most intense events are dominated more by these events than by the properties of relatively inert, truly isolated vortex tubes.

Two scenarios. What is different about this event than the usual scenario? Table I outlines two scenarios: one based on interacting antiparallel vortex tubes being the most intense structures, the other based on what is observed developing from smooth initial conditions such as Taylor-Green[3] interactions between vortex structures in fully developed turbulence[9] and here. In this scenario, antiparallel vortex structures are never observed and helicity clearly plays a major role.

What is the underlying origin of the differences between the two scenarios? All the calculations that lead to antiparallel configurations are inviscid, initialized either using vortex filaments and tubes (see Ref. 23, and references in Ref. 24). The spectral calculations reported here, which are viscous and initially develop vortex sheets, show no antiparallel trend. Since sheets do not have an axial direction along which vorticity will align, other alignments are possible and the growth of the large-scale helicity is also possible. The new mechanism does not appear to depend upon either the inviscid rollup of isolated vortex sheets or the reconnection of antiparallel vortices.

Nonetheless, two helical properties associated with antiparallel interactions are seen. At their point of closest ap-

proach, opposing ends of the interacting vortices generate helicity of opposite sign and when the vortex lines reconnect, it is the ends with oppositely signed helicity that connect. However, a major difference after reconnection begins, is that in an antiparallel configuration, the increase in dissipation is rather small.[25] The asymmetrical helicity interactions that are allowed in the present case appear to be intrinsically related to the fourfold increase in dissipation. From this calculation and earlier work,[19] it could be that a train of helicity fluctuations moving to small scales as in Fig. 7 is needed for there to be rapid dissipation. This could not occur if the vortices at the smallest scales were antiparallel.

Two final points about helicity. While the helicity density is not Galilean invariant, Galilean transformations could not remove the strong fluctuations in helicity in physical space that we observe, nor could they remove the strong fluctuations in the helicity cospectrum in Fig. 6. The implication is that if these are configurations that naturally and frequently arise in a turbulent flow, then helicity could be playing a central role in their dynamical evolution. The second point is that the interactions of oppositely signed helical are transients originating from an initial value problem and appear to enhance the turbulent cascade. Despite superficial similarities with the oscillations in helicity in the Glezder-Ohkitani-Yamada (GOY) shell model[26] that was discussed in an earlier paper,[19] we do not believe that a shell model is the correct description for the phenomena observed. In the GOY model, the helicity fluctuations play a role in producing an intermittent statistical state through blocking the cascade.[27]

A new twist. The three-dimensional graphics and helicity analysis presented provide evidence for a new coherent mechanism for the formation of dissipative structures characterized by viscous, transverse vortex sheets gradually transforming themselves into interacting, transverse vortex tubes, which are intrinsically helical. The transverse configuration forms during the period with the strongest surge in vorticity and is associated with strong fluctuations in the helicity in both physical and Fourier space. Viscous dissipation plays a role as early as $T=0.4$, but has not been visualized. One would expect sheets of dissipation as identified previously.[9] All of these observations would be consistent with earlier theoretical suggestions, that dissipative sheets could be separating regions of maximally positive and negative helicity,[28] and analysis of triad interactions, where oppositely signed helical modes enhance energy transfer.[29]

Only one idealized state has been considered here. How will this state determine the intermittent turbulent state that follows? Our approach to this problem will be to search large data sets for examples of what has been discussed, then see what develops. The tools developed here could help us identify the conditions under which the structures of fully developed turbulence appear.

ACKNOWLEDGMENTS

We are enormously grateful to our colleagues for their helpful constructive suggestions about how to present the extensive data file. In particular we thank the Turbulence Working Group at Los Alamos National Laboratory and C. Vassilicos at Imperial College. We acknowledge support of the Turbulence Working Group and the T-7 Group of the Theoretical Division at Los Alamos.

APPENDIX: DETAILS FOR $0.5<T<0.7$

The diagrams in Figs. 9–11 are designed to summarize how the sheets at $T=0.5$ have turned into tubular structures, how new alignments arise, and how helicity is transformed. In the diagrams three colors indicate the sign of helicity: Green for $h>0$, blue for $h<0$, and black for neutral helicity $h\sim 0$.

Referring to the steps in Sec. V:

Ends of oppositely signed helicity reconnect. Compare the upper-left diagram at $T=0.6$ in Fig. 10 with the left diagram at $T=0.5$ in Fig. 9. The parts that reconnect on the left are indicated by the red and blue arrows in the two diagrams. The green $h>0$ horizontal structure indicated by the blue arrow at $T=0.5$ has reconnected with the blue $h<0$ vertical structure indicated by the red arrow. This becomes in the $T=0.6$, $\theta_y=55$ diagram, a blue $h<0$ curved structure connected to the black $h\sim 0$ vertical structure. The parts that reconnect on the right are the green $h>0$ bottom of the underlying sheet at $T=0.5$ in Fig. 9 with the blue $h<0$ right-hand side of the overlying sheet of both the diagram and three-dimensional image in Fig. 9. There is only partial reconnection at $T=0.6$ with at least one vortex line still following its original path.

Further information on alignments is given by the other perspectives in Fig. 10. The perspective of the cube in Fig. 10 and the right picture at $T=0.5$ in Fig. 8 are between the $\theta_y=115$ and 175 perspectives of the cartoon in Fig. 10. The vertical isosurface near the yellow cross in the cube corresponds to the black twisting $h\sim 0$ vertical lines with the red arrow. The red cross in the cube corresponds to the straighter, more horizontal, black $h\sim 0$ structure.

Vortex tubes. The new structures at $T=0.6$ in the cube of Fig. 10 are more tube-like than the sheets in the two perspectives at $T=0.5$ in Fig. 8, which show the existence of sheets at $T=0.5$ best. In particular, the red arrows point to the same structure, which for $T=0.5$ in Fig. 8 is the vertical structure in the 50° perspective and the sheet-like structure that is bent far back in the 160° perspective. The sheet in the middle of the 50° perspective corresponds to the upper sheet in the 160° perspective and lies over the sheet indicated by the red arrow.

Helicity is neutralized. Note that despite the large vorticity in the upper left of the cube at $T=0.6$, helicity has almost disappeared in this region. This corresponds to the black $h\sim 0$ structures in the diagrams. The regions of $h\sim 0$ appear to develop because the polarized source term in (4) reverses sign after the direction of vorticity has changed.

New blue $h<0$ *structure appears*. The blue $h<0$ tip in the cube, and indicated by the blue arrows in the diagrams of Fig. 10, has formed from the green $h>0$ structure at $T=0.5$ in Fig. 9. The sign of helicity changes as this tip

snakes around the major green $h>0$ structure and appears to come from the flow of helicity from the vortex segment indicated by the red arrow that was blue ($h<0$) at $T=0.5$ and is black ($h\sim 0$) at $T=0.6$.

Opposite helicity vortex tubes at $T=0.7$. The blue tip at $T=0.6$ becomes the blue $h<0$ cross vortex at $T=0.7$ in Fig. 11. Eventually the entire structure is annihilated.

[1] In order to celebrate mathematics in the new millennium, the Clay Mathematics Institute of Cambridge, Massachusetts has named seven "prize" problems. The official Navier-Stokes problem asks for proof of one of four statements, all related to either existence and smoothness of the Navier-Stokes equations, or their breakdown in three dimensions. For further information, see *The Millennium Prize Problems*, edited by J. Carlson (Clay Mathematics Institute, Providence, RI 2005); URL: www.claymath.org/millennium/

[2] J. T. Beale, T. Kato, and A. Majda, "Remarks on the breakdown of smooth solutions of the 3-D Euler equations," Commun. Math. Phys. **94**, 61 (1984).

[3] M. E. Brachet, D. I. Meiron, S. A. Orszag, B. G. Nickel, R. H. Morf, and U. Frisch, "Small-scale structure of the Taylor-Green vortex," J. Fluid Mech. **130**, 411 (1983).

[4] M. E. Brachet, M. Meneguzzi, A. Vincent, H. Politano, and P. L. Sulem, "Numerical evidence of smooth self-similar dynamics and possibility of subsequent collapse for three-dimensional ideal flows," Phys. Fluids A **4**, 2845 (1992).

[5] R. M. Kerr, "Evidence for a singularity of the three-dimensional, incompressible Euler equations," Phys. Fluids A **5**, 1725 (1993).

[6] R. Grauer, C. Marliani, and K. Germaschewski, "Adaptive mesh refinement for singular solutions of the incompressible Euler equations," Phys. Rev. Lett. **80**, 4177 (1998).

[7] A. Brandenburg and R. M. Kerr, "Helicity in hydro and MHD reconnection," in *Quantized Vortex Dynamics and Superfluid Turbulence*, edited by C. F. Barenghi, R. S. Donnelly, and J. Vinen (Cambridge University Press, Cambridge, UK, 2001).

[8] E. D. Siggia, "Numerical study of small scale intermittency in three-dimensional turbulence," J. Fluid Mech. **107**, 375 (1981).

[9] R. M. Kerr, "Higher order derivative correlations and the alignment of small-scale structures in isotropic numerical turbulence," J. Fluid Mech. **153**, 31 (1985).

[10] A. Vincent and M. Meneguzzi, "The spatial structure and statistical properties of homogeneous turbulence," J. Fluid Mech. **225**, 1 (1991).

[11] G. Compte-Bellot and S. Corrsin, "Simple Eulerian time correlation of full- and narrow-band velocity signals in grid-generated, 'isotropic' turbulence," J. Fluid Mech. **48**, 273 (1971).

[12] J. R. Herring and R. M. Kerr, "Comparison of direct numerical simulation with prediction of two-point closures," J. Fluid Mech. **118**, 205 (1982).

[13] J. R. Herring and R. M. Kerr, "Development of enstrophy and spectra in numerical turbulence," Phys. Fluids A **5**, 2792 (1993).

[14] D. D. Holm and R. M. Kerr, "Transient vortex events in the initial value problem for turbulence," Phys. Rev. Lett. **88**, 244501 (2002).

[15] L. G. Margolin, P. K. Smolarkiewicz, and A. A. Wyszogradzki, "Implicit turbulence modeling for high Reynolds number flows," J. Fluids Eng. **124**, 862 (2002).

[16] D. Drikakis, "Advances in turbulent flow computations using high-resolution methods," Prog. Aerosp. Sci. **39**, 405 (2003).

[17] Unfortunately, the size of the peak, $H(k=6.5)$ at $t=0.7$ in our earlier work (Ref. 14), was an artifact of an FFT hardware error when analysis of a Cray-YMP calculation was done on a Cray-J9. The strong peak disappears after $t\approx 0.55$.

[18] R. M. Kerr, "Velocity and scaling of collapsing Euler vortices," Phys. Fluids **17**, 075103 (2005).

[19] L. Biferale and R. M. Kerr, "On the role of inviscid invariants in shell models of turbulence," Phys. Rev. E **52**, 6113 (1995).

[20] W. Polifke and L. Shtilman, "The dynamics of helical decaying turbulence," Phys. Fluids A **1**, 2025 (1989).

[21] A similar effect was found in a simulation of forced isotropic turbulence in energy transfer spectra. R. M. Kerr, "Velocity, scalar and transfer spectra in numerical turbulence," J. Fluid Mech. **211**, 309 (1990).

[22] Z.-S. She, E. Jackson, and S. A. Orszag, "Intermittent vortex structures in homogeneous isotropic turbulence," Nature (London) **344**, 226 (1990).

[23] A. Pumir and E. D. Siggia, "Vortex dynamics and the existence of solutions of the Navier-Stokes equations," Phys. Fluids **30**, 1606 (1987).

[24] S. Kida and M. Takaoka, "Vortex reconnection," Annu. Rev. Fluid Mech. **26**, 169 (1994).

[25] R. M. Kerr and F. Hussain, "Simulation of vortex reconnection," Physica D **37**, 474 (1989).

[26] L. Biferale, "Shell models of energy cascade in turbulence," Annu. Rev. Fluid Mech. **35**, 441 (2003).

[27] L. Kadanoff, D. Lohse, and J. Wang, "Scaling and dissipation in the shell GOY model," Phys. Fluids **7**, 617 (1995).

[28] H. K. Moffatt, "Magnetostatic equilibria and analogous Euler flows of arbitrarily complex topology. Part 1, fundamentals," J. Fluid Mech. **159**, 359 (1985).

[29] F. Waleffe, "Inertial transfers in the helical decomposition," Phys. Fluids A **5**, 677 (1993).